Since January 2020 Elsevier has created a COVID-19 resource centre with free information in English and Mandarin on the novel coronavirus COVID-19. The COVID-19 resource centre is hosted on Elsevier Connect, the company's public news and information website.

Science of the Total Environment 750 (2021) 141575

Contents lists available at ScienceDirect

Science of the Total Environment

journal homepage: www.elsevier.com/locate/scitotenv

Competing $PM_{2.5}$ and NO_2 holiday effects in the Beijing area vary locally due to differences in residential coal burning and traffic patterns

Jinxi Hua [a], Yuanxun Zhang [a,b,*], Benjamin de Foy [c], Xiaodong Mei [a], Jing Shang [a,d], Chuan Feng [c]

[a] College of Resources and Environment, University of Chinese Academy of Sciences, Beijing, China
[b] CAS Center for Excellence in Regional Atmospheric Environment, Chinese Academy of Sciences, Xiamen, China
[c] Department of Earth and Atmospheric Sciences, Saint Louis University, St. Louis, MO, USA
[d] Institute of Urban Meteorology, China Meteorological Administration, Beijing, China

HIGHLIGHTS

- During the holidays, $PM_{2.5}$ is about 22% higher and NO_2 is about 11% lower in the greater Beijing area.
- On Saturdays, $PM_{2.5}$ is about 4% lower and NO_2 is about 3% lower in downtown Beijing.
- On Sundays, $PM_{2.5}$ is about 5% higher but NO_2 is similar to weekdays.
- Holiday increases in $PM_{2.5}$ are about 18.4% larger in the southwest and northeast than in other rural areas.
- Suburban areas have larger holiday reductions in NO_2 than downtown areas.

GRAPHICAL ABSTRACT

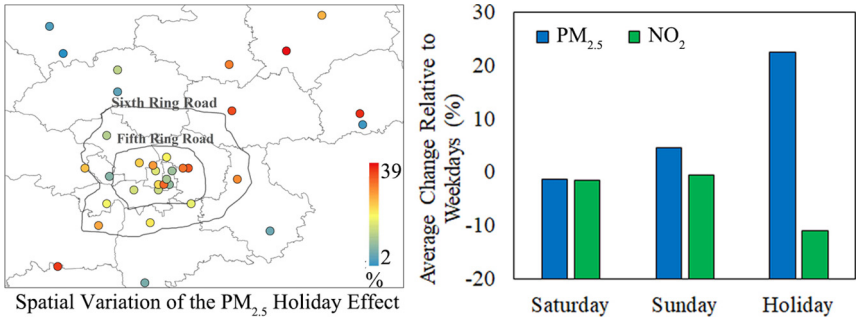

ARTICLE INFO

Article history:
Received 6 June 2020
Received in revised form 5 August 2020
Accepted 7 August 2020
Available online 11 August 2020

Editor: Pingqing Fu

Keywords:
Holiday effects
Traffic emissions
Residential coal burning
GAM analysis
Spatial variations

ABSTRACT

The holiday effect is a useful tool to estimate the impact on air pollution due to changes in human activities. In this study, we assessed the variations in concentrations of fine particulate matter ($PM_{2.5}$) and nitrogen dioxide (NO_2) during the holidays in the heating season from 2014 to 2018 based on daily surface air quality monitoring measurements in Beijing. A Generalized Additive Model (GAM) is used to analyze pollutant concentrations for 34 sites by comprehensively accounting for annual, monthly, and weekly cycles as well as the nonlinear impacts of meteorological factors. A Saturday effect was found in the downtown area, with about 4% decrease in $PM_{2.5}$ and 3% decrease in NO_2 relative to weekdays. On Sundays, the $PM_{2.5}$ concentrations increased by about 5% whereas there were no clear changes for NO_2. In contrast to the small effect of the weekend, there was a strong holiday effect throughout the region with average increases of about 22% in $PM_{2.5}$ and average reductions of about 11% in NO_2 concentrations. There was a clear geographical pattern in the strength of the holiday effect. In rural areas the increase in $PM_{2.5}$ is related to the proportion of coal and biomass consumption for household heating. In the suburban areas between the Fifth Ring Road and Sixth Ring Road there were larger reductions in NO_2 than downtown which might be due to decreased traffic as many people return to their hometown for the holidays. This study provides insights into the pattern of changes in air pollution due to human activities. By quantifying the changes, it also provides insights for improvements in air quality due to control policies implemented in Beijing during the heating season.

* Corresponding author at: College of Resources and Environment, University of Chinese Academy of Sciences, Beijing, China.
E-mail address: yxzhang@ucas.ac.cn (Y. Zhang).

https://doi.org/10.1016/j.scitotenv.2020.141575
0048-9697/

1. Introduction

The weekend effect refers to the difference in pollutant concentrations or meteorological parameters between weekdays and weekends (Beirle et al., 2003; Forster and Solomon, 2003). It is mainly due to changes in behavior from working on weekdays to resting on weekends. In the megacities of US, Europe, Japan, and Russia, air pollution weekend effects were identified by ground measurements and remote sensing, usually showing reductions of up to 50% or more during the weekends compared with weekdays (Beirle et al., 2003; de Foy et al., 2016a; de Foy and Schauer, 2019; Elansky et al., 2020; Marr and Harley, 2002; Motallebi et al., 2003). For the weekly cycle of Beijing, China, ozone (O_3) has been reported to have a clear weekly periodical variation with a maximum on weekends (Wang et al., 2013; Zhao et al., 2019). In contrast, for fine particles ($PM_{2.5}$) and nitrogen dioxide (NO_2), there have been conflicting results. Cui et al. (2020) found concentrations of thirteen elements in $PM_{2.5}$ were higher on weekends than on weekdays. (Beirle et al., 2003; Chen et al., 2015; Liu et al., 2016) did not find a clear weekly pattern in the Beijing area. These studies did not consider the effect of meteorology on pollutant concentrations. The regional transport plays an important role in the air pollution of Beijing: a clear spatial pattern was observed with decreasing concentrations from south to north (Li et al., 2015). Because meteorology has a strong impact on air pollution in the region, it must be taken into account to prevent biases in the estimates of human-related air pollution changes (Sun et al., 2013; Sun et al., 2015; Wang et al., 2017a; Wang et al., 2016).

In addition to meteorology, local emissions also affect air quality. The main anthropogenic sources of air pollution in Beijing during the heating season are coal-burning for heating and vehicle emissions due to rapid urbanization (Liu et al., 2018; Xu et al., 2019). A series of measures were implemented to improve air quality in the city, such as "Action Plan on Prevention and Control of Air Pollution" (Zhang et al., 2016), "Joint Prevention and Control of Atmospheric Pollution" (Wang and Zhao, 2018), "Coal to Electricity" and "Coal to Gas" projects (Shuxue et al., 2020). The actions have been found to effectively reduce the $PM_{2.5}$ and NO_2 concentrations (Barrington-Leigh et al., 2019; Cheng et al., 2019; de Foy et al., 2016b; Wang et al., 2017b; Zhang et al., 2018). Nevertheless, progress in clean energy development varies between urban and rural areas due to a variety of transportation and financial support factors. Coal was prohibited in Beijing within the Sixth Ring Road (Cai et al., 2018), but coal-based household heating is still an important emission source in rural areas during the past few years (Duan et al., 2014; Hua et al., 2018; Zhao et al., 2020c; Zhi et al., 2017).

The holiday effect is similar to the weekend effect in that it is a measure of the difference in pollution levels between holidays and non-holidays (Tan et al., 2013). In general, it shows higher concentrations during non-holidays and lower concentrations during holidays. The holiday effect is due to changes in human activities which are influenced by lifestyle, urbanization, energy consumption structure, and traditional culture (Forster and Solomon, 2003; Liu et al., 2019; Seidel and Birnbaum, 2015). When there is no clear weekend effect, the holiday effect provides a useful tool to identify changes in air quality due to changes in human activities (Chen et al., 2019). Madhavi Latha and Highwood (2006) found coarse particulate matter (PM_{10}) concentrations are lower during the Christmas holidays than non-holidays in the United Kingdom, which are mainly due to reductions of local traffic emissions. Chen et al. (2019) and Tan et al. (2009) investigated the difference of six air pollutants in Taipei between the Spring Festival and non-Spring Festival, finding significant reductions during the Spring Festival for nitrogen oxides (NO_x), carbon monoxide (CO), volatile organic compounds or non-methane hydrocarbon (NMHC), sulfur dioxide (SO_2), and PM_{10}, while O_3 concentrations increased due to a reduction in the titration effect. Tan et al. (2013) reported a distinct spatial holiday effect associated with the degree of urbanization in Taipei and found that the holiday effects of NO_x, CO and NMHC become greater when the population, and hence the number of motor vehicles increases.

Beijing, China has a population of more than 20 million inhabitants. During public holidays, more than 10% of the population travels away from the area (Pan and Lai, 2019). There are clear changes in sources during the holidays and non-holidays due to changes in human activities. During the Spring Festival, the most important traditional festival in China, a large number of people return to their hometowns to reunite with their families, and the traffic volume decreases significantly in megacities (Li et al., 2016; Zhang et al., 2015). At the same time, the coal and biomass combustion activities for heating and cooking increases (Feng et al., 2012; Wen et al., 2018). The larger changes in human behavior during the holidays can provide more information than the weekend effects (Chen et al., 2019), but existing research on human-related holiday effects of air quality in Beijing is missing.

Common methods used to explore the temporal pattern of air quality include Multiple Linear Regression (MLR) models and Generalized Additive Models (GAM) (Wood, 2000; Wood and Augustin, 2002). In general, the most relevant factors, such as time vectors and meteorological parameters, are used to identify the impact on $PM_{2.5}$ and NO_2 concentrations. MLR was applied to estimate temporal profiles of NO_x emissions in Chicago (de Foy, 2018), the variation of ozone, NO_x and $PM_{2.5}$ in Fresno (de Foy et al., 2020; de Foy and Schauer, 2019), the variations of NO_2 columns in China and American cities (de Foy et al., 2016a; de Foy et al., 2016b). The non-linear model GAM was used to assess changes of OMI NO_2 columns over Europe (Zhou et al., 2012).

A GAM was used to identify the temporal profiles of $PM_{2.5}$ and NO_2 caused by emissions changes with respect to the nonlinear impacts of meteorological parameters. The model was based on measurements during the heating season from 2014 to 2018 at 34 air quality monitoring stations in Beijing. The spatial variations of the temporal profiles are analyzed according to land-use characteristics.

2. Materials and methods

2.1. Air quality measurements

Hourly $PM_{2.5}$ and NO_2 measurements during the heating season (December to March) were collected from December 2014 to March 2019 for 34 sites (Fig. 1) in the Beijing area. The data was available from the Beijing Municipal Environmental Monitoring Center (http://www.bjmemc.com.cn/). These sites are designed to reflect urban background conditions, regional transmission, traffic pollution, and urban air quality, covering most of the spatial range and multiple land use types (Ji et al., 2019; Sun et al., 2019). For each site, daily averages were calculated from the valid data points when data was available for more than 10 h per day. The location of the sites and the number of observations as shown in Table S1. $PM_{2.5}$ and NO_2 were available for more than 95% of the days for most sites during the study period (756 days in total).

Beijing includes 16 administrative regions (Fig. 1), with a total population of 21.54 million in 2018 (Beijing Municipal Bureau of Statistics, 2019) and an area of 16,410km^2 (Dong et al., 2018). Rapid urbanization caused a drastic expansion from core districts (Dongcheng and Xicheng). The area within the Fifth Ring Road is considered the most densely populated area with around half of the inhabitants and only 4% of the surface area of Beijing (Beijing Bureau of Statistics and Beijing Survey Team of the National Bureau of Statistics; Dong et al., 2018). Due to relatively short commuting time and cheap housing, the area between the Fifth Ring Road and the Sixth Ring Road accounts for 27% of the population of Beijing City (Beijing Bureau of Statistics and Beijing Survey Team of the National Bureau of Statistics). Outside the Sixth Ring Road, the population density is relatively sparse, and rural residents account for a large proportion, with approximately 86% of land area only 24% of the population (Beijing Bureau of Statistics and Beijing Survey Team of the National Bureau of Statistics; Dong et al., 2018).

Different population distribution and development patterns will lead to variations in air pollution due to variations in human activities.

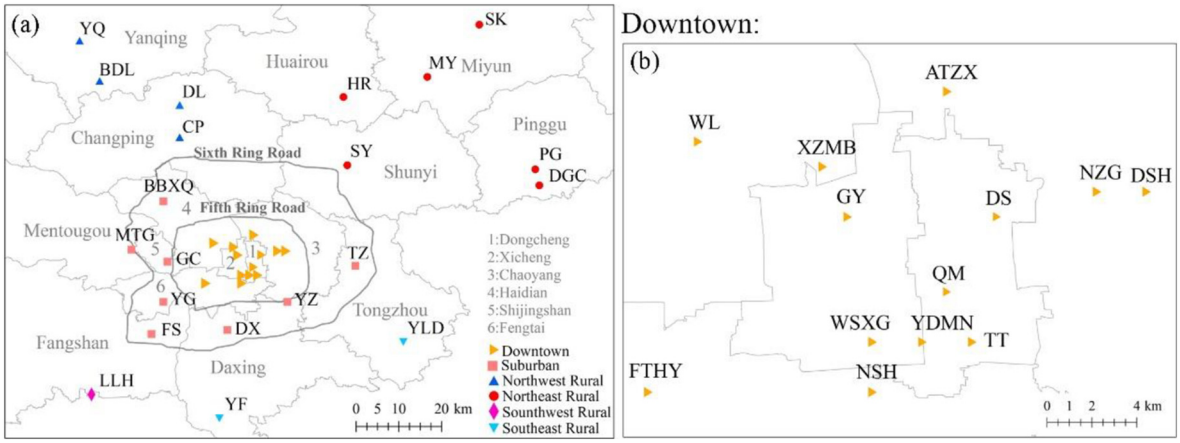

Fig. 1. (a): Map of air quality monitoring sites at Beijing denoting the geographical location groups. The sites within the Fifth Ring Road were defined as downtown, the sites between the Fifth Ring Road and the Sixth Ring Road as suburban, the sites outside the Sixth Ring Road as Rural areas. (b): Enlarged map of the downtown area.

To explore the spatial variation of the holiday effect, the sites were clustered by geographical locations based on different population and development patterns (Fig. 1). The sites within the Fifth Ring Road were defined as downtown, the sites between the Fifth Ring Road and the Sixth Ring Road were defined as suburban, the sites outside the Sixth Ring Road were defined as rural areas. Downtown includes ATZX, DSH, FTHY, GY, NSH, NZG, TT, WL, WSXG, XZMB, YDMN, DS, and QM. The suburban region contains BBXQ, GC, MTG, YG, DX, FS, YZ, and TZ. The rural area was separated into four sectors: HR, MY, SK, PG, SY, and DGC for the northeast, BDL, CP, YQ, and DL for the northwest, YF and YLD for the southeast, and LLH for the southwest.

2.2. Meteorological parameters

Surface meteorological parameters, including wind speed, wind direction, relative humidity (RH), air temperature at two meters above the surface (T2M), dew point temperature at two meters above the surface (D2M), and surface pressure (SP) were obtained from the Integrated Surface Data (ISD) from the National Oceanic and Atmospheric Administration (NOAA) (https://www.ncdc.noaa.gov/isd/data-access). The meteorological monitoring station was located at Beijing Capital International Airport (40.08°N, 116.585°E). The wind speed and wind direction were converted to the zonal velocity (U) and meridional velocity (V) as inputs to the GAM model. The daily average, minimum and maximum values of relative humidity, air temperature, dew point temperature, and pressure were calculated from hourly observations.

Boundary layer height (BLH) plays an important role in the pollution formation and dispersion at different temporal scales (Miao et al., 2019). In this study, hourly boundary layer height was available from fifth-generation atmospheric reanalysis dataset (ERA5) from the European Centre for Medium-Range Weather Forecasts (https://cds.climate.copernicus.eu/). The same meteorological variables as ISD were also obtained from ERA5 to perform preliminary tests. Linear interpolation was used to obtain 0.01° resolution raster from 0.25° original grids. The time of all data points is unified to China Standard Time (CST, UTC + 8).

2.3. Definition of holiday periods and Mann-Whitney U test

The holiday periods referred to New Year's Day (January 1), the Spring Festival (Lunar New Year), and the Lantern Festival based on the national legal holiday arrangements issued by the State Council. The Spring Festival is the most important holiday involving family reunions, and it will bring travel peaks of people returning to their hometowns before the festival and then back to work afterwards. For the purposes of this study, the Festival holiday period is defined as starting two days before the eve of the Spring Festival and finishing four days after the Spring Festival. This excludes the influence of the travel peaks which occur before and after that (Li et al., 2016). The specific dates are listed in Table S2. Overall, the holiday periods last around ten days each year.

In this study, the non-parametric Mann-Whitney U test, which does not require the data to be normally distributed (Chen et al., 2019), was used to compare the pollutant concentrations and meteorological observations during the holidays and non-holidays, weekends and weekdays.

2.4. Generalized Additive Model (GAM) analysis

The predictors in our GAM model (Wood, 2017) include time vectors to represent inter-annual, monthly, and weekday variations, as well as meteorological variables (boundary layer height, east-west wind component, south-north wind component, relative humidity, air temperature, dew point temperature, and surface pressure). The time factors were defined as linear terms, and the meteorological variables were defined as smooth terms. The equation is as follows:

$$\log(CONC + offset) = \sum_{yr=2014}^{2018} \alpha_{yr} t_{yr} + \sum_{m=Mar}^{NOV} \alpha_m t_m + \sum_{i=1}^{8} \alpha_{wkd_i} t_{wkd_i} + s_1(BLH) + s_2(U,V) + s_3(Optimized\ Input) + \alpha_{baseline} + \in \quad (1)$$

The dependent variables were logarithm transformed and used offset by 30 μg/m^3 for the daily concentration of NO_2 concentrations in order to approximate a normal distribution. α are the regression coefficients. $\alpha_{baseline}$ represents the baseline condition and ε are the residuals.

The categorical variables t represents the temporal scale by year, month, and day. The data points take a value one during the selected time period and zero otherwise. Inter-annual variations separated by heating season are represented by t_{yr} from 2014 to 2018. The monthly cycles t_{month} use five monthly indicators from November to March. The impact of week days is denoted by t_{wd} for each day of the week (Mondays, Tuesdays, Wednesdays, Thursdays, Fridays, Saturdays, Sundays) as well as for the Holidays.

S (·) is the P-spline smoothing function that optimizes the fitting and controls the smoothness through a penalty term. S_1 (BLH) are the smoothers that characterize the non-linear influence of boundary layer height on the measurements. S_2 (U, V) are interaction terms that denote the influence of horizontal ventilation due to zonal and meridional wind speeds. "*Optimized Input*" represent the meteorological variables selected in the candidate list based on their contribution to the model R^2. The candidate list included relative humidity, air temperature,

dew point temperature, and pressure. To avoid the collinearity problem, the test process input only one variable to GAM at a time. The one leading to the greatest increase in correlation coefficient was included. All meteorological variables were scaled linearly in order to approximate the normal distribution of zero mean to reduce the effects of extreme observations.

After considering the impact of meteorological parameters, a net contribution to the time cycle can be obtained from the regression coefficient. In this way, temporal profiles are closer to changes caused by emissions than meteorological factors. The temporal indicators are input for each year, each month, and each day of the week, and therefore do not have a unique solution. As described in (de Foy, 2018), a weighting factor of one was used on the penalty term for the regression coefficients which solves the dummy variable trap problem while also forcing α to have the smallest possible values.

The GAM results can be interpreted using Eq. (2):

$$p = (e^{\alpha} - 1) \times 100\% \quad (2)$$

where p corresponds to the percentage change in the concentration during the time intervals relative to long-term averages.

Block-bootstrapping (de Foy and Schauer, 2015; Requia et al., 2019) with seven-day chunks was used to estimate the uncertainty of the linear terms. The model was obtained 100 times using a randomly resampled dataset each time. When resampling the dataset, the data points to be included were selected at random with replacement so that each dataset was of the same size as the original. The standard deviation of the temporal coefficients was obtained from the 100 model simulations. The 95% confidence interval of the nonlinear terms in Eq. (1) can be obtained directly from gam function in the mgcv package (Wood, 2000; Wood and Augustin, 2002) in R environment (Version 3.6.3) (R Core Team, 2019).

3. Results and discussion

3.1. Characteristics of observations in holidays and non-holidays

Fig. 2 shows the day-to-day variations for $PM_{2.5}$ and NO_2 concentrations based on all the data points during the heating season from 2014 to 2018. During the non-holiday periods, it can be seen that the concentrations of pollutants are very similar from Mondays to Fridays, with an average level of 73-85 μg/m^3 for $PM_{2.5}$ and 53-55 μg/m^3 for NO_2. The pollutant concentrations are highest on Saturdays with 91 μg/m^3 $PM_{2.5}$ concentration and 59 μg/m^3 NO_2 concentration, respectively. There is no clear difference between Sundays and Weekdays. Compared with the average level from Mondays to Sundays, Holidays are clearly different, with 18% higher $PM_{2.5}$ and 20% lower NO_2 concentrations (Table 1). The mean (± SD) $PM_{2.5}$ concentrations are 96 ± 82 μg/m^3 and 81 ± 80 μg/m^3 in holidays and non-holidays, respectively. The mean (± SD) NO_2 concentrations are 44 ± 29 μg/m^3 and 55 ± 31 μg/m^3 during holidays and non-holidays, respectively.

Daily means of $PM_{2.5}$ and NO_2 between the holidays and non-holidays, weekends and weekdays periods were found to be statistically different with $p < .01$ using the Mann-Whitney U test (Table 1). Meteorological variables were also statistically different, which means that it was important to consider these factors in the model in order to properly quantify the human-related air pollution changes. During the holidays, the mean BLH is 47 m lower than non-holidays and the air temperature is around 3 °C lower. The main reason for the difference is that the holiday periods fall mainly within January and February which are colder than March. The same weather parameters from ERA5 and ISD show a consistent bias: BLH, D2M, T2M, RH, SP, and U are lower during the holidays and V is higher.

3.2. Model performance, meteorological impacts, and annual trends

The average standard deviations of $PM_{2.5}$ scaling factors are around 4.5% and 9.9% in non-holidays and holidays, respectively, and they are stable from site to site (Table S3). The relatively high uncertainty of holiday effects is due to the fact that there are fewer data points for the holiday periods than for the non-holidays. For NO_2, the uncertainty of non-holidays is around 1.5% and for holidays it is around 2.6%. The uncertainty for $PM_{2.5}$ is higher than NO_2 mainly because $PM_{2.5}$ concentrations are affected by complex factors such as various emission sources, air mass transport, chemical transformation, day-to-day carry over, and complex interaction effect between synoptic conditions and $PM_{2.5}$ (Wang et al., 2017a, b; Khuzestani et al., 2018).

The performance of the model fit was assessed by calculating the regression coefficient (r^2) and the Root Mean Square Error (RMSE) using the 100 bootstrap runs (Table 2). For $PM_{2.5}$, r^2 values varied from 0.72 to 0.79, and RMSE from 0.40 to 0.54 μg/m^3. For NO2, r^2 varied from 0.66 to 0.84, and RMSE varied from 0.13 μg/m^3 to 0.19 μg/m^3. The residuals were normally distributed for both $PM_{2.5}$ and NO_2 (examples shown in Fig. S1 and Fig. S2).

Overall, the GAM estimates of the holiday effects were found to be robust for each site with respect to the selection of the optimal set of meteorological variables.

The list of variables selected as input to the GAM for each site is shown in Table S1. Daily average boundary layer height and ISD winds were included in most cases, and the average relative humidity was

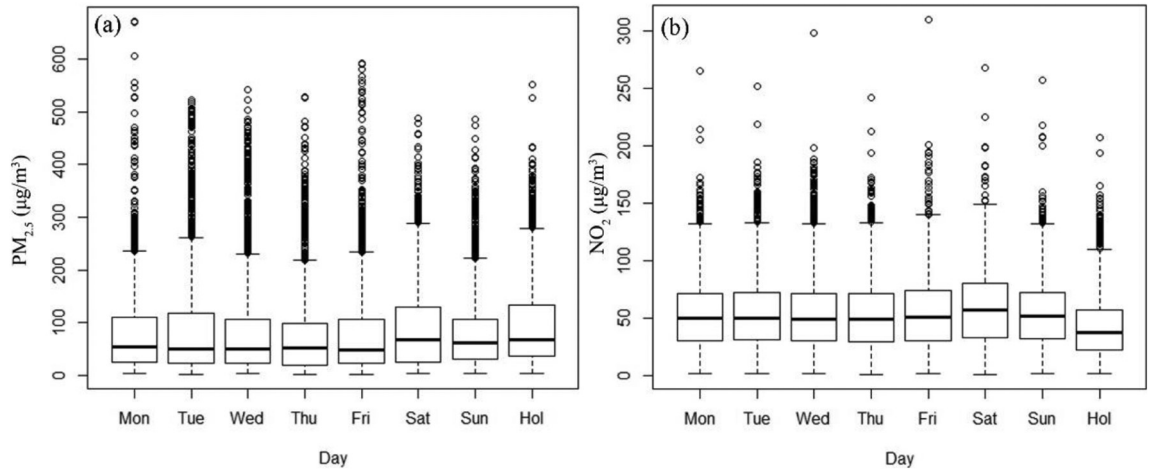

Fig. 2. Day of the week variations of daily $PM_{2.5}$ (a) and NO_2 (b) concentrations based on measurements during the heating season from 2014 to 2018. The bold black line represents the median, the box range is between 25% and 75% percentile of the dataset, the whiskers show 1.5 times the interquartile range away from the box, the hollow circles are outliers.

Table 1
Statistical characteristics of $PM_{2.5}$, NO_2, and meteorological parameters between holidays and non-holidays, weekends and weekdays. "Diff-Hol" are the median values in holiday periods minus non-holidays, "Diff-Day" are the median values in weekend periods minus weekdays, and *** denotes the statistically significant difference ($p < .01$) from the Mann-Whitney *U* test.

	Units	Non-holidays	Holidays	Diff-Hol	Weekdays	Weekends	Diff-Day
$PM_{2.5}$	μg/m^3	81.2 ± 80.0	95.9 ± 82.0	12.4***	80.6 ± 81.0	87.0 ± 78.0	11.0***
NO_2	μg/m^3	54.8 ± 31.4	43.9 ± 28.5	−13.2***	53.1 ± 31.2	56.9 ± 31.5	5.6***
ERA5 BLH	m	438.0 ± 306.0	391.0 ± 224.0	−3.3***	442.5 ± 299.1	416.8 ± 314.7	−54.9***
ISD D2M	°C	−11.1 ± 7.8	−13.9 ± 6.5	−2.3***	−11.6 ± 7.7	−10.3 ± 7.7	2.5***
ERA5 D2M	°C	−11.2 ± 8.0	−14.3 ± 7.2	−3.3***	−11.8 ± 8.0	−10.5 ± 8.0	2.5***
ISD T2M	°C	2.1 ± 5.4	−0.7 ± 3.0	−2.1***	1.8 ± 5.3	2.2 ± 5.6	0.9***
ERA5 T2M	°C	0.1 ± 5.2	−1.4 ± 2.7	−1.0***	0.5 ± 5.1	1.0 ± 5.2	0.5***
ISD RH	%	43.8 ± 19.3	42.5 ± 18.6	−4.6***	42.9 ± 19.0	45.8 ± 19.8	3.1***
ERA5 RH	%	45.3 ± 17.3	42.1 ± 17.9	−5.2***	44.3 ± 17.0	47.3 ± 18.1	4.2***
ISD SP	h Pa	1026.0 ± 7.0	1026.0 ± 7.0	−2.0***	1026.2 ± 6.9	1025.6 ± 6.5	−1.0***
ERA5 SP	h Pa	1010.0 ± 18.0	1010.0 ± 18.0	−0.8	1009.9 ± 17.8	1009.4 ± 17.6	−0.5***
ISD U	m/s	0.6 ± 1.6	0.3 ± 1.2	−0.2***	0.6 ± 1.5	0.5 ± 1.6	−0.1***
ERA5 U	m/s	0.4 ± 0.9	0.2 ± 0.9	−0.2***	0.4 ± 0.9	0.4 ± 1.0	−0.1***
ISD V	m/s	−1.1 ± 1.9	−0.9 ± 1.5	0.1***	−1.2 ± 1.9	−1.0 ± 1.8	0.2***
ERA5 V	m/s	−0.5 ± 1.2	−0.4 ± 1.0	0.1***	−0.5 ± 1.2	−0.5 ± 1.1	0.1***

the optimal choice at the majority of sites during the sensitivity tests. We will take the site YZ as an example to discuss the impact of meteorology on pollutant concentrations. The site is located in the plain area and near a subway station, which means that its topographic features are similar to most of the other sites and it is strongly impacted by human activities. The increase in the mixing layer height led to the strong diffusion of pollutants (Miao et al., 2019), leading to approximately a 65% decrease in $PM_{2.5}$ with one standard deviation increase in the boundary layer height at YZ (Fig. S3). High relative humidity promotes the hygroscopic growth of particulate matter (Cheng et al., 2015), with about a 65% increase in $PM_{2.5}$ with one standard deviation increase in the relative humidity. Beijing is surrounded by mountains to the west, north, and northeast; and the southeast is a plain that slopes slowly towards the Bohai Sea. Because of the topographical features, the air quality at most sites is influenced by southerly winds. Frequent northerly winds during the heating periods also transport air pollution from downtown to YZ site which is a suburban site to the southeast. For NO_2, an increase in one standard deviation of the boundary layer height is associated with a 22% decrease at YZ (Fig. S4). Higher relative humidity is associated with higher NO_2 concentrations. Except for the

Table 2
The GAM analysis performance and average relative changes in Weekdays, Saturdays, Sundays, and Holidays compared to weekdays for $PM_{2.5}$ and NO_2 at each site.

Sites	$PM_{2.5}$					NO_2				
	R^2	RMSE (μg/m^3)	Saturday (%)	Sunday (%)	Holiday (%)	R^2	RMSE (μg/m^3)	Saturday (%)	Sunday (%)	Holiday (%)
ATZX[1]	0.77	0.46	−5.21	1.71	22.81	0.81	0.15	−2.92	−1.26	−11.95
DSH[1]	0.79	0.46	−3.23	4.53	27.11	0.82	0.13	−1.87	−1.17	−11.55
FTHY[1]	0.76	0.47	−4.14	8.31	21.89	0.80	0.13	−3.02	−0.79	−11.62
GY[1]	0.77	0.46	−5.12	4.01	22.04	0.82	0.14	−3.05	−0.78	−10.87
NSH[1]	0.78	0.46	−4.08	6.24	21.71	0.78	0.12	−3.57	−1.13	−9.60
NZG[1]	0.77	0.47	−2.95	5.03	26.88	0.83	0.14	−2.05	−0.80	−12.21
TT[1]	0.77	0.47	−2.63	7.66	20.44	0.81	0.13	−2.38	−0.80	−10.43
WL[1]	0.78	0.46	−2.92	3.67	23.68	0.82	0.14	−2.77	−1.16	−9.89
WSXG[1]	0.77	0.47	−2.89	4.50	23.08	0.84	0.13	−2.91	−0.28	−11.00
XZMB[1]	0.77	0.43	−3.49	2.59	25.26	0.81	0.13	−3.90	−0.65	−9.58
YDMN[1]	0.77	0.46	−3.94	4.83	26.95	0.79	0.15	−4.06	−1.04	−11.33
DS[1]	0.77	0.48	−5.53	4.14	20.53	0.82	0.13	−2.95	−1.75	−12.47
QM[1]	0.77	0.44	−4.57	3.77	20.60	0.82	0.14	−2.54	−0.09	−8.57
BBXQ[2]	0.79	0.44	−1.16	3.01	20.89	0.80	0.16	−1.41	−1.55	−15.74
GC[2]	0.78	0.44	−4.93	2.46	19.48	0.83	0.14	−2.77	−1.72	−14.38
MTG[2]	0.76	0.46	−2.00	2.86	24.46	0.82	0.14	−2.59	−0.54	−11.99
YG[2]	0.77	0.45	−2.66	4.50	22.49	0.76	0.17	−1.12	1.05	−12.42
DX[2]	0.78	0.46	−0.68	5.17	22.86	0.81	0.14	−0.69	−0.95	−12.16
FS[2]	0.78	0.44	−1.92	5.00	25.09	0.80	0.14	−1.50	−0.55	−12.23
YZ[2]	0.77	0.49	−1.33	6.93	22.11	0.79	0.14	−0.73	−0.51	−15.51
TZ[2]	0.77	0.48	1.16	6.73	25.69	0.73	0.18	0.10	−2.00	−8.31
HR[3-1]	0.76	0.48	−0.73	1.05	26.43	0.76	0.14	−1.21	−1.45	−7.29
MY[3-1]	0.74	0.48	−0.79	−0.57	38.51	0.77	0.14	−2.23	−1.30	−7.14
SK[3-1]	0.72	0.54	1.21	9.55	25.05	0.66	0.15	−0.08	0.38	−3.65
PG[3-1]	0.75	0.47	2.78	5.14	34.85	0.80	0.13	0.65	−0.38	−8.27
SY[3-1]	0.75	0.48	4.30	5.35	28.49	0.81	0.14	−0.93	−1.90	−9.66
DGC[3-1]	0.75	0.48	4.94	9.71	10.71	0.71	0.19	0.66	5.52	−7.36
BDL[3-2]	0.76	0.40	−2.22	8.51	2.50	0.76	0.14	0.14	1.56	−17.40
CP[3-2]	0.78	0.42	−0.66	1.19	14.17	0.80	0.14	−1.87	−1.16	−13.56
YQ[3-2]	0.77	0.41	2.04	5.65	11.83	0.77	0.14	0.70	−0.17	−15.89
DL[3-2]	0.79	0.46	−0.70	2.73	21.04	0.81	0.16	0.08	−0.48	−7.69
YF[3-3]	0.73	0.45	1.76	7.07	17.42	0.73	0.15	−0.77	−0.55	−11.88
YLD[3-3]	0.77	0.44	4.83	6.76	15.01	0.77	0.14	1.27	−0.55	−14.24
LLH[3-4]	0.74	0.42	−0.86	1.38	30.34	0.75	0.14	0.06	0.50	−7.64

[1]The sites located in downtown area. [2] The sites located in suburban area. [3-1] The sites located in northeast rural area. [3-2] The sites located in northwest rural area. [3-3] The sites located in southeast rural area. [3-4] The sites located in southwest rural area.

influence from southerly winds, local emissions were found to have high contributions to NO_2 levels because the YZ site is very busy as it is near a subway station.

The 95% confidence interval range is very narrow for the meteorological parameters (Fig. S3 and Fig. S4) suggesting that the estimate of the impacts is robust. At the extremes, the uncertainty ranges are wider, although this is mostly because there are fewer data points on the edges of the distribution.

The year to year variations of concentrations, annual profiles and spatial variations are provided in Fig. S5- Fig. S7. In 2014, the mean scale factor was 36% above baseline concentrations whereas it was 10% lower than the baseline in 2018. For NO_2, the concentrations were 8% higher in 2014 and 6% lower in 2018 relative to the baseline, corresponding to around 14% in reduction over 6 years. The clear downward trend from 2014 to 2018 shows the effectiveness of the implementation of a series of emission control policies in Beijing over the past few years (Zhang et al., 2016). The maximum difference between 2014 and 2018 of $PM_{2.5}$ levels mainly occurred in the southern regions outside of the Fifth Ring Road where there is a high density of factories and more local emissions than in the northern regions (Xue et al., 2016). The area with high-intensity NO_2 emission reductions is mostly near to downtown, nevertheless there are a few sites (e.g. LLH, YLD) in the southern rural area that have about 5% per year reductions, which is probably due to tight emissions standards and declining heavy-duty truck traffic for goods transportation during recent years (Hua et al., 2018; Zhang et al., 2014).

3.3. Day of the week patterns

For the day of the week profiles, the $PM_{2.5}$ scaling factors vary from site to site, but on average there is not much variation from Monday to Sunday (Fig. 3, Table 2). Averaged across all sites, the day of week factors from Mondays to Sundays vary only from −5% to 2% for $PM_{2.5}$ and from 0% to 2.5% for NO_2. For downtown sites, concentrations on Saturdays are approximately 4% lower for $PM_{2.5}$ and 3% lower for NO_2 relative to weekdays. On Sundays, the concentrations are about 5% higher for $PM_{2.5}$, but there is no clear difference for NO_2 compared to weekdays. The signal of $PM_{2.5}$ and NO_2 on weekends are consistent at all downtown sites (Fig. S8) suggesting that the weekend effects are robust with respect to spatial variability. The weekend effect in $PM_{2.5}$ can be clearly seen even though $PM_{2.5}$ is influenced by carry over on the scale of 3 to 5 days. While this shows that the weekend effect is strong enough to be identified over other factors, future analysis would be required to estimate the impacts of carry over, for example using aerosol chemical speciation. The probability distribution of percentage changes by type of day shows that the differences between the days are statistically significant. As an example, the distributions of $PM_{2.5}$ factors at WSXG are clearly different for Saturdays, Sundays and Holidays, and the distributions of NO_2 factors are clearly different for Saturdays and Holidays (Fig. S9). This result updates the previous research on the weekend effect in Beijing. (Beirle et al., 2003; Chen et al., 2015; Liu et al., 2016) which showed that there was no obvious weekend effect for $PM_{2.5}$ or NO_2 in Beijing, mainly because the previous study mostly did not consider the impact of meteorological parameters and of spatial patterns. This implies that the GAM analysis provides valuable information with respect to temporal variation and meteorological influence, and that a network of widely distributed monitoring stations can provide more subtle information on the weekend effect.

A clear difference between holidays and non-holidays can be seen, and the change has opposite signs for $PM_{2.5}$ and NO_2. Relative to weekdays, $PM_{2.5}$ was about 22.4% higher while NO_2 was about 11.0% lower during the holiday periods. The opposite holiday effects for $PM_{2.5}$ and NO_2 suggest that there are multiple factors involved in the change of human-activities, as will be discussed in Section 3.4.

3.4. Spatial patterns of holiday effects

From downtown to suburban, to rural areas, there is a clear change in the holiday effects in the direction of a larger increase of $PM_{2.5}$ and a smaller decrease of NO_2 (Fig. 4). For the most part, sites in close geographical proximity behave similarly, although there are a few outliers. DL, DGC, and TZ exhibit different characteristics from the neighboring sites, probably because they are affected by local land use effects. For example, DGC is geographically close to PG, but DGC is surrounded by farmland and forest while PG is located in a residential area (Fig. S10), which suggests that the different holiday effects are due to local variations in land use type. DL was purposely designed to monitor urban background air quality surrounded by mountainous areas (Chen et al., 2015; Li et al., 2015). These sites are excluded in the analysis that follows.

For downtown, the changes are relatively consistent, with an increase in $PM_{2.5}$ concentrations ranging from 20.4% to 27.1% and a reduction in NO_2 ranging from 8.6% to 12.5% (Table 2). For most sites in the suburban region, the $PM_{2.5}$ changes are close to downtown sites with 19.5– 25.1% increases, and the changes in NO_2 are stronger than downtown with 12.0– 15.7% decreases.

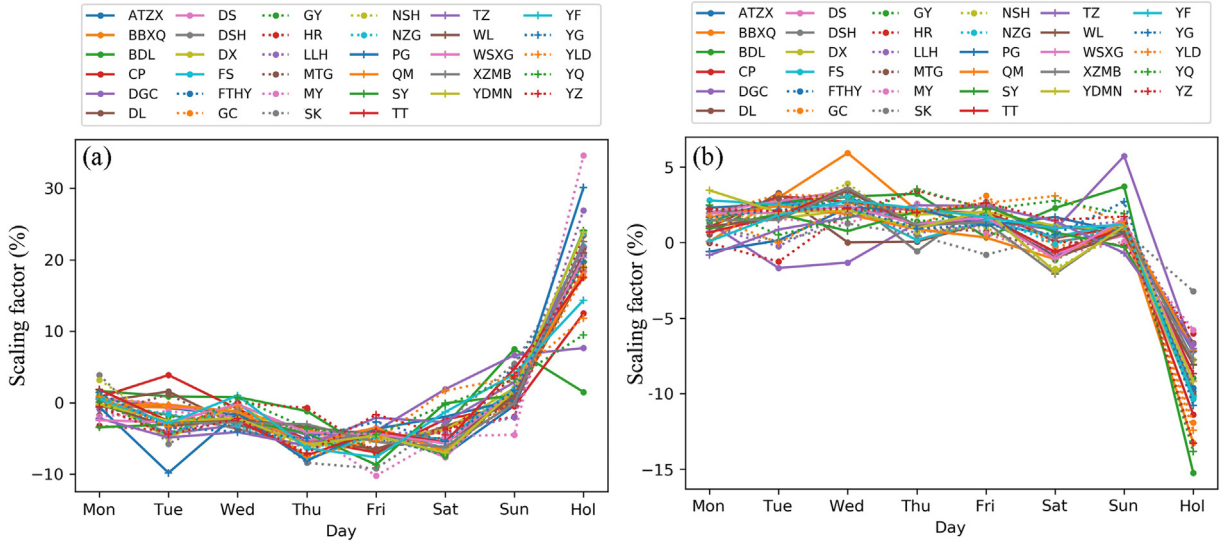

Fig. 3. Weekly profiles in $PM_{2.5}$ (a) and NO_2 (b) for 34 sites based on scaling factors from the GAM analysis. The factors represent the percentage change relative to long-term averages.

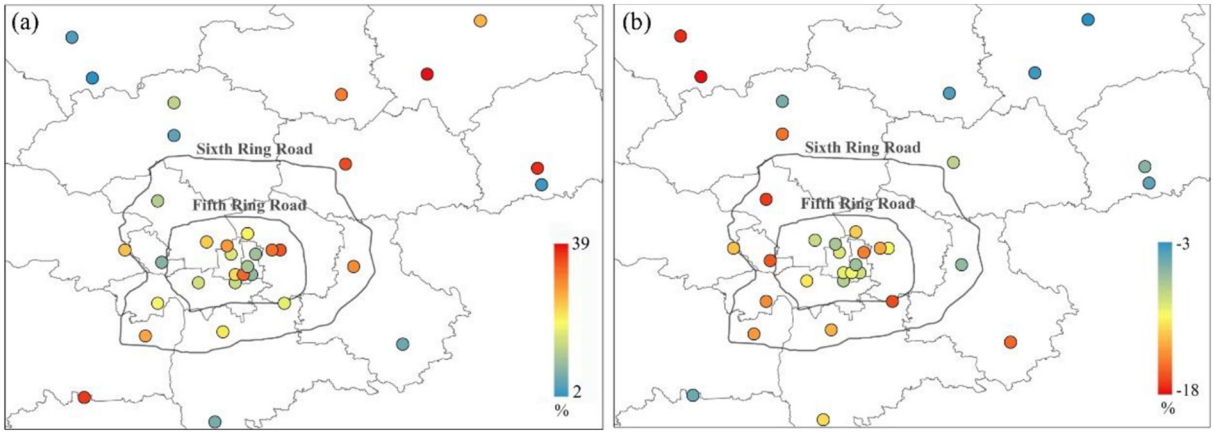

Fig. 4. Spatial variations of holiday effects compared to weekdays for $PM_{2.5}$ (a) and NO_2 (b) at each site from 2014 to 2018. The colors from blue to red indicate the amplitudes of $PM_{2.5}$ increase or NO_2 reduction from low to high.

The effects of holidays in rural areas are clearly distinct. For the $PM_{2.5}$ holiday effect, the southwest and northeast rural areas demonstrate the largest increases, being on average 30.6% higher than weekdays. The sites in the southeast and northwest areas show the lowest increases with 12.2% changes on average. This pattern is similar to the feature of $PM_{2.5}$ emissions from household heating in Cai et al. (2018), who developed a village-based emission inventory of household combustion based on the investigation of all villages in Beijing. For NO_2, the sites in the southwest and northeast rural areas have the lowest decrease (7.3% on average) while the sites in the southeast and northwest areas have the highest decrease (14.6% on average).

3.5. Influences on the holiday effects

The $PM_{2.5}$ holiday effect consisted of increased concentrations ranging from 2% to 39% depending on the site. In contrast, the NO_2 holiday effect consisted of decreased concentrations ranging from 3% to 18% depending on the site. That $PM_{2.5}$ has a stronger holiday effect than NO_2 implies that there are greater differences in human activities for $PM_{2.5}$ emission sources.

Rural areas to the northeast of Beijing experienced larger increases in $PM_{2.5}$ concentrations. These are mainly concentrated in Miyun, Huairou, and Pinggu, which are districts in northeast Beijing and are more heavily forested, and where coal and biomass burning is frequently used as a heating fuel (Cai et al., 2018). Yuan et al. (2015) found that coal-fired boilers have been mostly eliminated from urban areas but remain in rural areas and especially in the districts of Miyun, Huairou, and PingGu in 2014.

We compared the strength of the holiday effect with household energy consumption by town in most districts of Beijing in 2017 provided by Cai et al. (2018). For each rural measurement site, we calculated the average coal and biomass consumption in neighboring districts. The strength of the holiday effect in $PM_{2.5}$ in rural areas was found to have a positive correlation with coal and biomass consumption (Fig. 5). The northeast and southwest rural areas had a higher proportion of coal consumption for household heating than the northwest and southeast rural areas, and had a correspondingly larger increase in $PM_{2.5}$ concentrations during the holidays. The spatial variation of the holiday effect suggests that indoor household heating activities could be a possible cause for the increases in $PM_{2.5}$ in rural areas. The results suggest that the promotion of the "coal to gas" project (Barrington-Leigh et al., 2019; Zhao et al., 2020b) will play an important role in improving air quality in Beijing in the next few years.

Household heating is also a significant source of NO_2 emissions (Luo et al., 2019), such that the NO_2 emitted by coal combustion probably

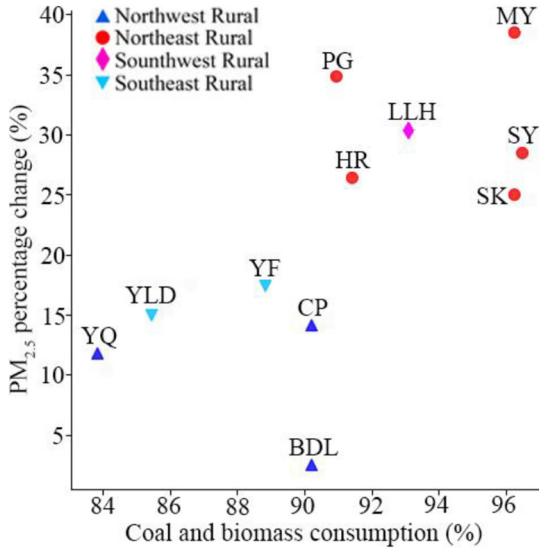

Fig. 5. The relationship between coal/biomass consumption for household heating and $PM_{2.5}$ percentage changes relative to weekdays for the sites located in the rural areas.

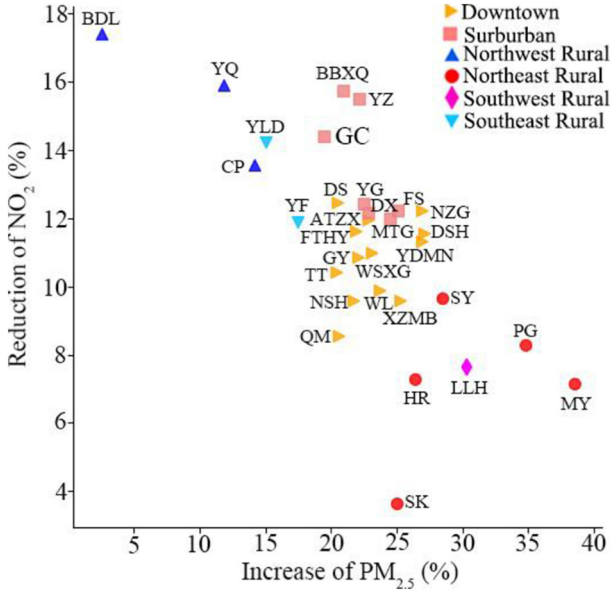

Fig. 6. Scatter plot of the $PM_{2.5}$ and NO_2 holiday effects at all the sites in the study. The marker types denote the different geographical groups.

offset the reduction of NO_2 due to reduced traffic. The area with more coal-fired activities have a smaller reduction in NO_2 than the areas with lower coal-fired activities. Therefore, the net NO_2 holiday effect in rural areas is a result of two competing effects. For the area within the Sixth Ring Road, although suburban areas and downtown show similar $PM_{2.5}$ increases, the suburban area exhibited an extra 2.7% reduction in NO_2 relative to the downtown area (Fig. 6). The difference is probably because the suburban area is home to a large number of commuters thanks to relatively cheap housing costs and short commute times, and consequently has a greater fraction of people traveling during the holidays (Zhao et al., 2020a). Changes in travel patterns are particularly strong during the Spring Festival when a large number of people return to their hometown leading to reduced transportation emissions during the Spring Festival itself. To distinguish between the effect of different holidays it will be necessary to have a longer time series of measurements.

4. Conclusions

In this study, we used GAM to estimate the holiday effects of $PM_{2.5}$ and NO_2 in Beijing by considering the time and meteorological factors at 34 different sites during the five heating seasons from December 2014 to March 2019. The difference in concentrations during holidays and non-holidays is a result of changes in both anthropogenic emissions and meteorological conditions. In order to properly quantify the human-related air pollution changes, it is important to consider the meteorological factors. By accounting for horizontal and vertical dispersion, it is possible to get a closer estimate of changes in emissions than would be possible by considering only changes in concentrations. The results showed a Saturday effect for the downtown area with about 4% and 3% reductions in $PM_{2.5}$ and NO_2 than weekdays. On Sundays, the $PM_{2.5}$ concentrations increased by about 5% whereas there were no clear changes for NO_2. Although there is uncertainty due to meteorological factors such as temperature, wind speed and direction, and boundary layer height, the weekend variations are consistent at all downtown sites and robust with respect to temporal variability. The holiday effect was found to be much stronger than the weekend effects, and had opposite signs for $PM_{2.5}$ and NO_2. There were increases in $PM_{2.5}$ ranging from 2% to 30% depending on the site. In contrast, NO_2 decreased from 3% to 18% depending on the site.

Furthermore, a clear spatial pattern was found in the strength of the holiday effect. In the rural areas, the strength of the $PM_{2.5}$ increases were associated with the extent of coal and biomass consumption for household heating in districts surrounding the measurement sites. It is worth noting that the promotion of renewable energy can therefore be expected to improve air quality in rural hotspots as well as in the greater Beijing area. In addition, the suburban area where more people travelled during the holidays experienced greater reductions in NO_2 than the downtown area. The spatial variation in the holiday effect at different sites reflects two distinct ways that human activities impact air quality: increased residential heating tended to increase both $PM_{2.5}$ and NO_2, whereas reduced traffic emissions leads to lower NO_2.

This study investigated the holiday effect in Beijing, providing evidence for the influence of human activities on air quality on short time scales. Studies of the holiday effects as well as other natural experiments such as the impacts of the Olympic games (Liu et al., 2012), APEC Blue (Gao et al., 2017; Sun et al., 2016), and new studies emerging on the impact of the COVID-19 lockdown (Bauwens et al., 2020; Chauhan and Singh, 2020; Wang and Su, 2020) will provide valuable information for the formulation of policies for both holiday and non-holiday periods.

CRediT authorship contribution statement

Jinxi Hua: Conceptualization, Data analysis, Visualization, Writing - original draft. **Yuanxun Zhang**: Supervision, Funding acquisition, Writing - review & editing. **Benjamin de Foy**: Conceptualization, Data analysis, Writing - review & editing. **Xiaodong Mei**: Writing - review & editing. **Jing Shang**: Writing - review & editing. **Chuan Feng**: Data analysis.

Declaration of competing interest

The authors declare that they have no known competing financial interests or personal relationships that could have appeared to influence the work reported in this paper.

Acknowledgements

This work was supported by the National Natural Science Foundation of China (NSFC, No. 41877310), partly by the National Key Research and Development Program of China (No. 2016YFC0503600) and the China Scholarship Council.

Appendix A. Supplementary data

Supplementary data to this article can be found online at https://doi.org/10.1016/j.scitotenv.2020.141575.

References

Barrington-Leigh, C., Baumgartner, J., Carter, E., Robinson, B.E., Tao, S., Zhang, Y., 2019. An evaluation of air quality, home heating and well-being under Beijing's programme to eliminate household coal use. Nat. Energy 4, 416–423.

Bauwens, M., Compernolle, S., Stavrakou, T., Müller, J.F., Gent, J., Eskes, H., et al., 2020. Impact of coronavirus outbreak on NO2 pollution assessed using TROPOMI and OMI observations. Geophys. Res. Lett. 47, e2020GL087978.

http://tjj.beijing.gov.cn/zt/rkjd/sdjd/201603/t20160322_143414.html (Accessed 21 May 2015).

Beijing Municipal Bureau of Statistics, 2019. Beijing regional statistical yearbook 2019. http://202.96.40.155/nj/qxnj/2019/zk/indexch.htm.

Beirle, S., Platt, U., Wenig, M., Wagner, T., 2003. Weekly cycle of NO2 by GOME measurements: a signature of anthropogenic sources. Atmos. Chem. Phys. 3, 2225–2232.

Cai, S., Li, Q., Wang, S., Chen, J., Ding, D., Zhao, B., et al., 2018. Pollutant emissions from residential combustion and reduction strategies estimated via a village-based emission inventory in Beijing. Environ. Pollut. 238, 230–237.

Chauhan, A., Singh, R.P., 2020. Decline in PM2.5 concentrations over major cities around the world associated with COVID-19. Environ. Res. 187, 109634.

Chen, W., Tang, H., Zhao, H., 2015. Diurnal, weekly and monthly spatial variations of air pollutants and air quality of Beijing. Atmos. Environ. 119, 21–34.

Chen, P.-Y., Tan, P.-H., Chou, C.C.K., Lin, Y.-S., Chen, W.-N., Shiu, C.-J., 2019. Impacts of holiday characteristics and number of vacation days on "holiday effect" in Taipei: implications on ozone control strategies. Atmos. Environ. 202, 357–369.

Cheng, Y., He, K.B., Du, Z.Y., Zheng, M., Duan, F.K., Ma, Y.L., 2015. Humidity plays an important role in the PM2.5 pollution in Beijing. Environ. Pollut. 197, 68–75.

Cheng, N., Cheng, B., Li, S., Ning, T., 2019. Effects of meteorology and emission reduction measures on air pollution in Beijing during heating seasons. Atmospheric Pollution Research 10, 971–979.

Cui, Y., Ji, D., He, J., Kong, S., Wang, Y., 2020. In situ continuous observation of hourly elements in PM2.5 in urban Beijing, China: occurrence levels, temporal variation, potential source regions and health risks. Atmos. Environ. 222, 117164.

de Foy, B., 2018. City-level variations in NOx emissions derived from hourly monitoring data in Chicago. Atmos. Environ. 176, 128–139.

de Foy, B., Schauer, J.J., 2015. Origin of high particle number concentrations reaching the St. Louis, Midwest supersite. J. Environ. Sci. 34, 219–231.

de Foy, B., Schauer, J.J., 2019. Changes in speciated PM2.5 California, due to NOx concentrations in Fresno, reductions and variations in diurnal emission profiles by day of week. Science of the Anthropocene 7, 45.

de Foy, B., Lu, Z., Streets, D.G., 2016a. Impacts of control strategies, the great recession and weekday variations on NO 2 columns above North American cities. Atmos. Environ. 138, 74–86.

de Foy, B., Lu, Z., Streets, D.G., 2016b. Satellite NO2 retrievals suggest China has exceeded its NOx reduction goals from the twelfth Five-Year Plan. Sci. Rep. 6, 35912.

de Foy, B., Brune, W.H., Schauer, J.J., 2020. Changes in ozone photochemical regime in Fresno, California from 1994 to 2018 deduced from changes in the weekend effect. Environ. Pollut. 263, 114380.

Dong, R., Zhang, Y., Zhao, J., 2018. How green are the Streets within the sixth ring road of Beijing? An analysis based on tencent street view pictures and the green view index. Int. J. Environ. Res. Public Health 15.

Duan, X., Jiang, Y., Wang, B., Zhao, X., Shen, G., Cao, S., et al., 2014. Household fuel use for cooking and heating in China: results from the first Chinese environmental exposure-related human activity patterns survey (CEERHAPS). Appl. Energy 136, 692–703.

Elansky, N.F., Shilkin, A.V., Ponomarev, N.A., Semutnikova, E.G., Zakharova, P.V., 2020. Weekly patterns and weekend effects of air pollution in the Moscow megacity. Atmos. Environ. 224, 117303.

Feng, J., Sun, P., Hu, X., Zhao, W., Wu, M., Fu, J., 2012. The chemical composition and sources of PM2.5 during the 2009 Chinese New Year's holiday in Shanghai. Atmos. Res. 118, 435–444.
Forster, P.M., Solomon, S., 2003. Observations of a "weekend effect" in diurnal temperature range. Proc. Natl. Acad. Sci. U. S. A. 100, 11225–11230.
Gao, M., Liu, Z., Wang, Y., Lu, X., Ji, D., Wang, L., et al., 2017. Distinguishing the roles of meteorology, emission control measures, regional transport, and co-benefits of reduced aerosol feedbacks in "APEC Blue". Atmos. Environ. 167, 476–486.
Hua, Y., Wang, S., Jiang, J., Zhou, W., Xu, Q., Li, X., et al., 2018. Characteristics and sources of aerosol pollution at a polluted rural site southwest in Beijing, China. Sci. Total Environ. 626, 519–527.
Ji, W., Wang, Y., Zhuang, D., 2019. Spatial distribution differences in PM2.5 concentration between heating and non-heating seasons in Beijing, China. Environ. Pollut. 248, 574–583.
Khuzestani, R.B., Schauer, J.J., Shang, J., Cai, T., Fang, D., Wei, Y., 2018. Source apportionments of PM2.5 organic carbon during the elevated pollution episodes in the Ordos region, Inner Mongolia, China. Environ. Sci. Pollut. Res. Int. 25, 13159–13172.
Li, R., Li, Z., Gao, W., Ding, W., Xu, Q., Song, X., 2015. Diurnal, seasonal, and spatial variation of PM 2.5 in Beijing. Science Bulletin 60, 387–395.
Li, J., Ye, Q., Deng, X., Liu, Y., Liu, Y., 2016. Spatial-temporal analysis on spring festival travel rush in China based on multisource big data. Sustainability 8, 1184.
Liu, Y., He, K., Li, S., Wang, Z., Christiani, D.C., Koutrakis, P., 2012. A statistical model to evaluate the effectiveness of PM2.5 emissions control during the Beijing 2008 Olympic Games. Environ. Int. 44, 100–105.
Liu, J., Li, J., Li, W., 2016. Temporal patterns in fine particulate matter time series in Beijing: a calendar view. Sci. Rep. 6, 32221.
Liu, Y., Yan, C., Zheng, M., 2018. Source apportionment of black carbon during winter in Beijing. Sci. Total Environ. 618, 531–541.
Liu, Q., Baumgartner, J., Schauer, J.J., 2019. Source apportionment of fine-particle, water-soluble organic nitrogen and its association with the inflammatory potential of lung epithelial cells. Environmental Science & Technology 53, 9845–9854.
Luo, L., Wu, Y., Xiao, H., Zhang, R., Lin, H., Zhang, X., et al., 2019. Origins of aerosol nitrate in Beijing during late winter through spring. Sci. Total Environ. 653, 776–782.
Madhavi Latha, K., Highwood, E.J., 2006. Studies on particulate matter (PM10) and its precursors over urban environment of Reading, UK. J. Quant. Spectrosc. Radiat. Transf. 101, 367–379.
Marr, L.C., Harley, R.A., 2002. Modeling the effect of weekday-weekend differences in motor vehicle emissions on photochemical air pollution in Central California. Environmental science & technology 36, 4099–4106.
Miao, Y., Li, J., Miao, S., Che, H., Wang, Y., Zhang, X., et al., 2019. Interaction between planetary boundary layer and PM2.5 pollution in megacities in China: a review. Current Pollution Reports 5, 261–271.
Motallebi, N., Tran, H., Croes, B.E., Larsen, L.C., 2003. Day-of-week patterns of particulate matter and its chemical components at selected sites in California. J. Air Waste Manage. Assoc. 53, 876–888.
Pan, J., Lai, J., 2019. Spatial pattern of population mobility among cities in China: case study of the National day plus mid-autumn festival based on Tencent migration data. Cities 94, 55–69.
R Core Team, 2019. R: A Language and Environment for Statistical Computing. R Foundation for Statistical Computing, Vienna, Austria.
Requia, W.J., Jhun, I., Coull, B.A., Koutrakis, P., 2019. Climate impact on ambient PM2.5 elemental concentration in the United States: a trend analysis over the last 30years. Environ. Int. 131, 104888.
Seidel, D.J., Birnbaum, A.N., 2015. Effects of Independence Day fireworks on atmospheric concentrations of fine particulate matter in the United States. Atmos. Environ. 115, 192–198.
Shuxue, X., Yueyue, W., Jianhui, N., Guoyuan, M., 2020. 'Coal-to-electricity' project is ongoing in north China. Energy 191, 116525.
Sun, Y., Wang, Z., Fu, P., Jiang, Q., Yang, T., Li, J., et al., 2013. The impact of relative humidity on aerosol composition and evolution processes during wintertime in Beijing, China. Atmos. Environ. 77, 927–934.
Sun, Y.L., Wang, Z.F., Du, W., Zhang, Q., Wang, Q.Q., Fu, P.Q., et al., 2015. Long-term real-time measurements of aerosol particle composition in Beijing, China: seasonal variations, meteorological effects, and source analysis. Atmos. Chem. Phys. 15, 10149–10165.
Sun, Y., Wang, Z., Wild, O., Xu, W., Chen, C., Fu, P., et al., 2016. "APEC Blue": secondary aerosol reductions from emission controls in Beijing. Sci. Rep. 6, 20668.
Sun, J., Gong, J., Zhou, J., Liu, J., Liang, J., 2019. Analysis of PM2.5 pollution episodes in Beijing from 2014 to 2017: classification, interannual variations and associations with meteorological features. Atmos. Environ. 213, 384–394.
Tan, P.-H., Chou, C., Liang, J.-Y., Chou, C.C.K., Shiu, C.-J., 2009. Air pollution "holiday effect" resulting from the Chinese New Year. Atmos. Environ. 43, 2114–2124.
Tan, P.-H., Chou, C., Chou, C.C.K., 2013. Impact of urbanization on the air pollution "holiday effect" in Taiwan. Atmos. Environ. 70, 361–375.
Wang, Q., Su, M., 2020. A preliminary assessment of the impact of COVID-19 on environment - a case study of China. Sci. Total Environ. 728, 138915.
Wang, H., Zhao, L., 2018. A joint prevention and control mechanism for air pollution in the Beijing-Tianjin-Hebei region in China based on long-term and massive data mining of pollutant concentration. Atmos. Environ. 174, 25–42.
Wang, Y.H., Hu, B., Wang, Y.S., 2013. Ozone weekend effects in the Beijing–Tianjin–Hebei metropolitan area, China. Atmospheric Chemistry and Physics Discussions 13, 13045–13078.
Wang, Y., de Foy, B., Schauer, J.J., Olson, M.R., Zhang, Y., Li, Z., et al., 2017a. Impacts of regional transport on black carbon in Huairou, Beijing, China. Environ. Pollut. 221, 75–84.
Wang, Y., Xue, Y., Tian, H., Gao, J., Chen, Y., Zhu, C., et al., 2017b. Effectiveness of temporary control measures for lowering PM2.5 pollution in Beijing and the implications. Atmos. Environ. 157, 75–83.
Wang, Y., Zhang, Y., Schauer, J.J., de Foy, B., Guo, B., Zhang, Y., 2016. Relative impact of emissions controls and meteorology on air pollution mitigation associated with the Asia-Pacific Economic Cooperation (APEC) conference in Beijing, China. Sci. Total Environ. 571, 1467–1476.
Wen, J., Shi, G., Tian, Y., Chen, G., Liu, J., Huang-Fu, Y., et al., 2018. Source contributions to water-soluble organic carbon and water-insoluble organic carbon in PM2.5 during Spring Festival, heating and non-heating seasons. Ecotoxicol. Environ. Saf. 164, 172–180.
Wood, S.N., 2000. Modelling and smoothing parameter estimation with multiple quadratic penalties. Journal of the Royal Statistical Society. Series B (Statistical Methodology) 62, 413–428.
Wood, S.N., 2017. Generalized Additive Models: An Introduction with R. Chapman and Hall/CRC.
Wood, S.N., Augustin, N.H., 2002. GAMs with integrated model selection using penalized regression splines and applications to environmental modelling. Ecol. Model. 157, 157–177.
Xu, Q., Wang, S., Jiang, J., Bhattarai, N., Li, X., Chang, X., et al., 2019. Nitrate dominates the chemical composition of PM2.5 during haze event in Beijing, China. Sci. Total Environ. 689, 1293–1303.
Xue, Y., Zhou, Z., Nie, T., Wang, K., Nie, L., Pan, T., et al., 2016. Trends of multiple air pollutants emissions from residential coal combustion in Beijing and its implication on improving air quality for control measures. Atmos. Environ. 142, 303–312.
Yuan, S., Xu, W., Liu, Z., 2015. A study on the model for heating influence on PM2.5 emission in Beijing China. Procedia Engineering 121, 612–620.
Zhang, S., Wu, Y., Wu, X., Li, M., Ge, Y., Liang, B., et al., 2014. Historic and future trends of vehicle emissions in Beijing, 1998–2020: a policy assessment for the most stringent vehicle emission control program in China. Atmos. Environ. 89, 216–229.
Zhang, J., Wu, L., Yuan, F., Dou, J., Miao, S., 2015. Mass human migration and Beijing's urban heat island during the Chinese New Year holiday. Science Bulletin 60, 1038–1041.
Zhang, H., Wang, S., Hao, J., Wang, X., Wang, S., Chai, F., et al., 2016. Air pollution and control action in Beijing. J. Clean. Prod. 112, 1519–1527.
Zhang, X., Zhang, W., Lu, X., Liu, X., Chen, D., Liu, L., et al., 2018. Long-term trends in NO2 columns related to economic developments and air quality policies from 1997 to 2016 in China. Sci. Total Environ. 639, 146–155.
Zhao, X., Zhou, W., Han, L., 2019. Human activities and urban air pollution in Chinese mega city: an insight of ozone weekend effect in Beijing. Physics and Chemistry of the Earth, Parts A/B/C 110, 109–116.
Zhao, P., Liu, D., Yu, Z., Hu, H., 2020a. Long commutes and transport inequity in China's growing megacity: new evidence from Beijing using mobile phone data. Travel Behav. Soc. 20, 248–263.
Zhao, S., Hu, B., Gao, W., Li, L., Huang, W., Wang, L., et al., 2020b. Effect of the "coal to gas" project on atmospheric NOX during the heating period at a suburban site between Beijing and Tianjin. Atmos. Res. 241, 104977.
Zhao, X., Zhao, X., Liu, P., Ye, C., Xue, C., Zhang, C., et al., 2020c. Pollution levels, composition characteristics and sources of atmospheric PM2.5 in a rural area of the North China Plain during winter. Journal of Environmental Sciences.
Zhi, G., Zhang, Y., Sun, J., Cheng, M., Dang, H., Liu, S., et al., 2017. Village energy survey reveals missing rural raw coal in northern China: significance in science and policy. Environ. Pollut. 223, 705–712.
Zhou, Y., Brunner, D., Hueglin, C., Henne, S., Staehelin, J., 2012. Changes in OMI tropospheric NO2 columns over Europe from 2004 to 2009 and the influence of meteorological variability. Atmos. Environ. 46, 482–495.